














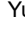



RESEARCH ARTICLE | DECEMBER 12 2023

Investigation of vertical GaN-on-GaN *p-n* diode with regrown *p*-GaN for operation in Venus and other extreme environments

Special Collection: [\(Ultra\)Wide-bandgap Semiconductors for Extreme Environment Electronics](#)

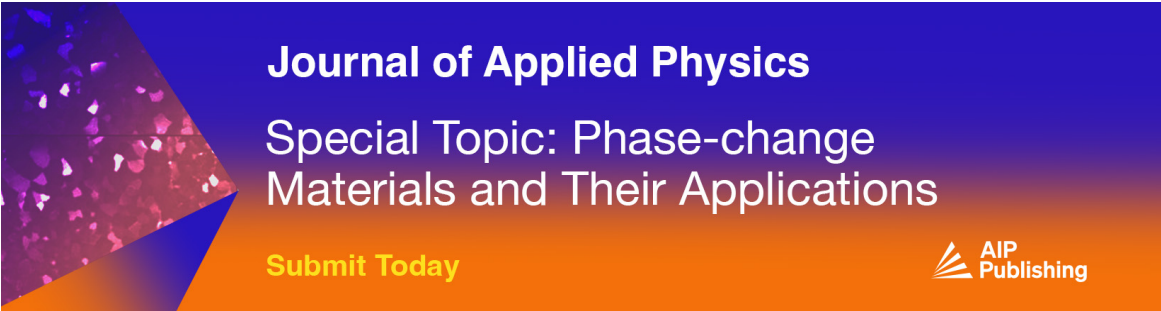
Shisong Luo ; Kai Fu ✉; Qingyun Xie ; Mengyang Yuan ; Guanhui Gao ; Hua Guo ; Rui Xu ; Noah Giles ; Tao Li ; Zhaobo Mei ; Mingfei Xu ; Jingan Zhou ; Ziyi He ; Cheng Chang ; Hanyu Zhu ; Tomás Palacios ; Yuji Zhao ✉

 Check for updates


Appl. Phys. Lett. 123, 243504 (2023)
<https://doi.org/10.1063/5.0173535>



CrossMark



Journal of Applied Physics
Special Topic: Phase-change Materials and Their Applications
[Submit Today](#)



Investigation of vertical GaN-on-GaN p - n diode with regrown p -GaN for operation in Venus and other extreme environments

Cite as: Appl. Phys. Lett. **123**, 243504 (2023); doi: [10.1063/5.0173535](https://doi.org/10.1063/5.0173535)

Submitted: 22 August 2023 · Accepted: 18 November 2023 ·

Published Online: 12 December 2023



View Online



Export Citation



CrossMark

Shisong Luo,¹ Kai Fu,^{1,2,3,a)} Qingyun Xie,⁴ Mengyang Yuan,⁴ Guanhui Gao,⁵ Hua Guo,⁵ Rui Xu,⁶ Noah Giles,¹ Tao Li,¹ Zhaobo Mei,¹ Mingfei Xu,¹ Jingan Zhou,^{1,2} Ziyi He,² Cheng Chang,¹ Hanyu Zhu,⁶ Tomás Palacios,⁴ and Yuji Zhao^{1,2,a)}

AFFILIATIONS

¹Department of Electrical and Computer Engineering, Rice University, Houston, Texas 77005, USA

²School of Electrical, Computer, and Energy Engineering, Arizona State University, Tempe, Arizona 85287, USA

³Department of Electrical and Computer Engineering, University of Utah, Salt Lake City, Utah 84112, USA

⁴Microsystems Technology Laboratories, Massachusetts Institute of Technology, Cambridge, Massachusetts 02139, USA

⁵Shared Equipment Authority, Rice University, Houston, Texas 77005, USA

⁶Department of Materials Science and Nanoengineering, Rice University, Houston, Texas 77005, USA

Note: This paper is part of the APL Special Collection on (Ultra)Wide-bandgap Semiconductors for Extreme Environment Electronics.

a) Authors to whom correspondence should be addressed: kai.fu@utah.edu and yuji.zhao@rice.edu

ABSTRACT

This Letter reports the performance of vertical GaN-on-GaN p - n diodes with etch-then-regrown p -GaN after exposure to a simulated Venus environment (460 °C, ~94 bar, containing CO₂/N₂/SO₂ etc., atmosphere) for over 10 days, and compared them to the performance of GaN p - n diodes without the etch-then-regrow process. After the above-mentioned Venus test, temperature-dependent I - V and microscopy investigation were conducted to study the robustness of etch-then-regrow p -GaN and vertical GaN p - n diodes under harsh environments and operation up to 500 °C. p -electrode degradation is found to be the main issue of the device's performance. This is the highest temperature at which such characterization has been conducted for vertical GaN p - n diodes, therefore establishing a critical reference for the development of p -GaN regrown and vertical GaN-based electronics for extreme environments.

Published under an exclusive license by AIP Publishing. <https://doi.org/10.1063/5.0173535>

Electronics operating in extreme environments are important in many industrial applications and outer space exploration.¹ Many applications (e.g., electrified automotive transportation and electric aircraft) of extreme environment electronics involve high power management.^{2,3} Compared with silicon, GaN is a promising solution for the operation of electronic devices in extreme environments due to its superior thermal, electrical, and chemical properties.⁴⁻⁶ For power electronics, GaN vertical devices already show excellent performance at room temperature and standard environmental conditions, because they offer a higher breakdown voltage for a given device footprint, higher current density, and lower dislocation density.⁷⁻⁹ Due to their potentially superior immunity to surface degradation and enhanced thermal management, GaN vertical power devices are promising for operation in extreme environments.¹⁰⁻¹²

A major challenge for GaN vertical devices is the formation of local GaN p - n junctions, which are critical building blocks for both devices and edge terminations.¹³ Selective area regrowth has been demonstrated to be a promising technology for fabricating patterned GaN p - n junctions. Dry etching before regrowth is necessary for forming selectively regrown areas, which is referred to as the etch-then-regrow process in this paper. In the past few years, researchers have extensively analyzed the etch-then-regrow process and related power devices.¹⁴⁻²¹ Therefore, it is worth studying the performance of GaN vertical power devices with etch-then-regrow p -GaN operation in extreme environments.

This Letter presents progress in vertical GaN power devices in the following aspects: (1) experiment of the properties of vertical GaN-on-GaN p - n diodes with regrown p -GaN operation up to 500 °C after over 10 days' simulated Venus environment exposure; (2) with

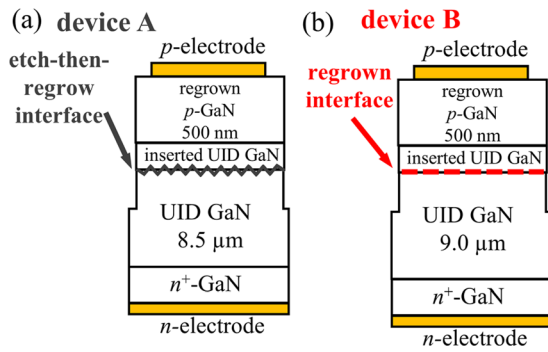


FIG. 1. Schematic cross section of (a) device A with the etch-then-regrow process and (b) device B with the regrown process.

electrical characterization and microscopy investigation, we demonstrated the robustness of regrown *p*-GaN and discovered that *p*-electrode degradation is the main degradation mechanism for such devices after extreme environment exposure. This is the highest temperature at which such characterization has been conducted for vertical GaN *p*-*n* diodes. These results are an important reference for GaN vertical power devices' operation in extreme environments with high temperature, high pressure, and corrosive gas.

Figure 1 shows the vertical GaN-on-GaN *p*-*n* diode structures used in this study. Epitaxy layers were grown by metalorganic chemical vapor deposition (MOCVD) on *c*-plane *n*⁺-GaN free-standing substrates with a Si doping concentration of $\sim 10^{18} \text{ cm}^{-3}$. 9- μm -thick unintentionally doped (UID) GaN drift layers were first grown on the substrates. A chlorine-based inductively coupled plasma (ICP) dry

etching recipe was used for device A's 500-nm-thick GaN etching (ICP/RF power = 400/75 W, pressure = 5 mTorr, $\text{Cl}_2/\text{BCl}_3/\text{Ar} = 32/8/5 \text{ sccm}$). For device B, no such dry etching process was used, and it was placed in a plastic sample container for a couple of days before regrowing *p*-GaN. Both samples are cleaned in an ultrasonication bath of acetone, isopropanol, and de-ionized water, respectively, and then re-loaded into the MOCVD chamber. A thin UID GaN layer was grown by MOCVD as an insertion layer followed by a 500 nm *p*-GaN layer. The source materials for Ga and N were, respectively, TMGa and NH_3 . The precursor for *p*-type dopants was Cp_2Mg . Then, mesa isolation was performed using dry etching technology. Metal stacks of Pd/Ni/Au (20/30/50 nm) were deposited by electron-beam evaporation and then annealed at 400 °C for 5 min in N_2 ambient to form an Ohmic contact to the *p*-GaN.²² Metal stacks of Ti/Al/Ni/Au (20/130/50/150 nm) were deposited to form a backside Ohmic contact. The properties of regrown *p*-GaN before exposure to harsh environments have been characterized by atomic force microscopy, x-ray diffraction, electroluminescence, secondary-ion-mass spectrometry (SIMS), transmission electron microscopy (TEM), scanning Kelvin probe force microscopy and scanning capacitance microscopy in the authors' previous report.^{23–27} According to the SIMS results, the Mg dopant's concentration in regrown *p*-GaN is on the order of 10^{19} – 10^{20} cm^{-3} , while the Si dopant's concentration in UID GaN is on the order of 10^{15} – 10^{16} cm^{-3} .^{23,24} These SIMS results has been used in the calculation of hole concentration [Fig. 2(h)], and the calculation methods are based on the charge neutrality condition.^{28,29}

The devices were placed in a simulated Venus environment (460 °C, ~ 94 bar, mainly CO_2/N_2 , traces of SO_2 atmosphere) over 10 days in the NASA Glenn Extreme Environment Rig (GEER).³⁰ The temperature and pressure conditions during the Venus test is

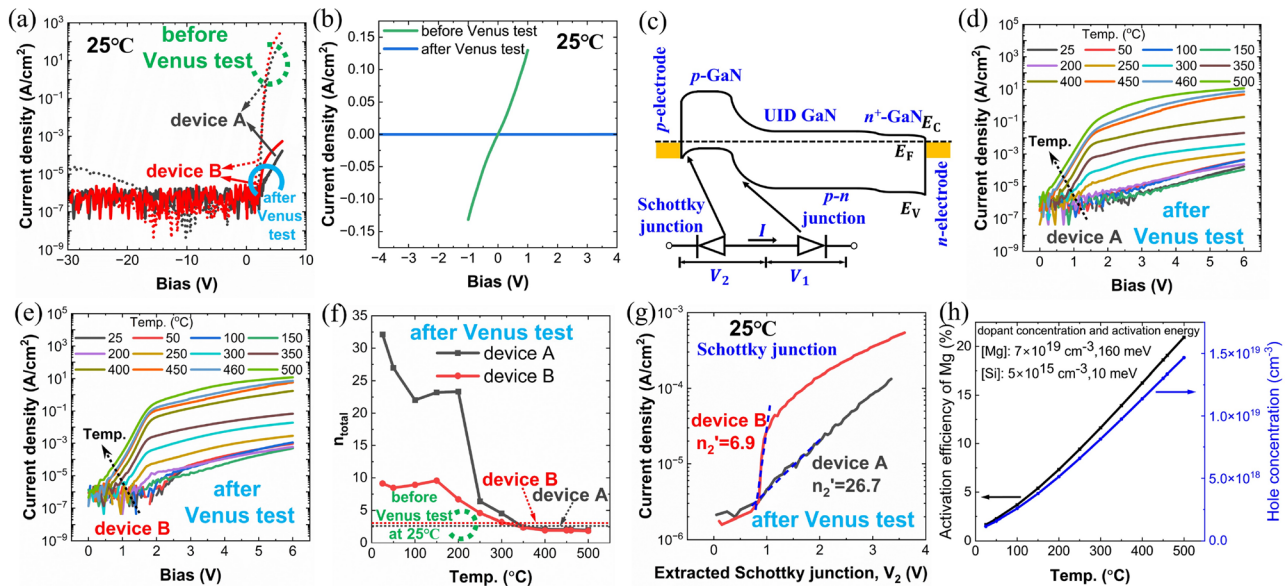


FIG. 2. (a) *J*-*V* curves of devices A and B at 25 °C. (b) *J*-*V* between two *p*-electrodes on *p*-GaN at 25 °C. (c) Top: schematic of the energy band structure in the devices without bias. Bottom: schematic of the equivalent circuit consisting of two diodes with bias. Forward bias *J*-*V* curves at 25–500 °C after the Venus test for (d) device A and (e) device B. (f) Total ideality factor as functions of temperature. (g) Extracted *J*-*V* characteristic of Schottky junction based on data in (a). (h) Calculated activation efficiency of Mg and hole concentration at 25–500 °C in regrown *p*-GaN.

described in our previous work,³¹ where the variation of temperature is less than 0.3 °C and that of pressure is less than 0.65 bar. After stressing the devices in a Venus-like atmosphere, the devices were characterized by a temperature-dependent I - V test. Figure 2(a) shows a dramatic decrease in forward current after exposure to the simulated Venus environment for both devices. Furthermore, we found nonlinear, asymmetric, and low-magnitude I - V curves between two p -electrodes on p -GaN, presenting a Schottky contact characteristic after the Venus test [Fig. 2(b)]. Therefore, a Schottky/ p - n diode model is proposed to explain the devices' dramatic decrease in forward current and high ideality factor after the Venus test [Fig. 2(c)]. This model assumes that the contact between p -electrode and p -GaN is a Schottky contact, and that the p -GaN, p -GaN/ n -GaN interface, n -GaN and n -GaN/ n -electrode contact does not change obviously after the passive test. The p - n diode I - V characteristics can approximate to $I_1 = I_{S1} \exp(qV_1/n_1kT)$. For p -electrode/ p -GaN junction, it could be treated as a Schottky diode under reverse bias. Since the current has a strong dependence both on temperature and voltage [Figs. 2(d) and 2(e)], the reverse current is expressed as $I_2 = I_{S2} \exp(qV_2/n_2'kT)$ in the thermionic-field emission regime.³² We have

$$n_2' = (1 - n_2^{-1})^{-1}, \quad (1)$$

where n_2' and n_2 are the ideality factor for reverse and forward bias, respectively. Therefore, the I - V characteristics of the devices under forward bias could be expressed as

$$\ln I = \frac{qV}{n_{\text{tot}}kT} + \frac{n_1 \ln I_{S1} + n_2' \ln I_{S2}}{n_{\text{tot}}}, \quad (2)$$

where $n_{\text{tot}} = n_1 + n_2'$, named as total ideality factor.

Fitting the curves in Figs. 2(c) and 2(d), the temperature-dependent total ideality factor is attained [Fig. 2(e)]. After the Venus test, n_{tot} decreases dramatically in the range of room temperature to 300 °C and then remains close to 2.0 for both device A and device B at temperatures higher than 300 °C. Based on Fig. 2(a), I - V characteristic of Schottky junction is extracted [Fig. 2(g)]. The n_2' is 26.7 for device A and 6.9 for device B at 25 °C after the Venus test. This p -electrode/ p -GaN Schottky contact could explain such anomalously high ideality factors at temperatures below 200 °C after the Venus test. Due to the higher thermal activation of acceptors in p -GaN at higher temperature [Fig. 2(h)], the contacts between p -electrode/ p -GaN display more Ohmic behavior. Consequently, n_2' and n_{tot} decrease rapidly. The same trend has been reported in similar GaN p - n junctions.³³

A microscopy investigation of device A was conducted after the above-mentioned test. Excellent crystal quality was observed in the p -GaN regrown on the etched surface. The contact morphology with the same anneal recipe for similar devices without harsh environment exposure has been reported.^{22,24} Compared with the p -GaN's TEM before the Venus test as reported in our previous work,²⁵ no noticeable degradation was found in the etched surface [Figs. 3(a) and 3(c)–3(e)], which demonstrates the robustness of etch-than-regrown p -GaN operation in extreme environments. Meanwhile, p -electrode degradation is discovered. The profile of metal elements is different from that of the annealed p -electrode without the simulated Venus environment exposure.^{34,35} The Pd/Ni/Au metal stack of p -electrode occurred interdiffusion and was deformed and oxidized. Au and Pd were mutually dissolved, and sulfur elements could also be found on the top of

the electrode [Figs. 3(f)–3(h)], indicating that sulfur from the SO₂ reacted with Pd during the simulated Venus environment exposure. A similar phenomenon has been reported in the Pt/Au electrode after exposure to the simulated Venus environment.^{36,37} The existence of sulfur could also explain the black color of p -electrode under optical microscopy [Fig. 3(b)]. Ni sinks to the bottom of the electrode and is oxidized [Figs. 3(f)–3(h)]. These degradations of p -electrode might severely affect the Ohmic contact with p -GaN. In summary, the microscopy investigation indicates the Schottky contact after the

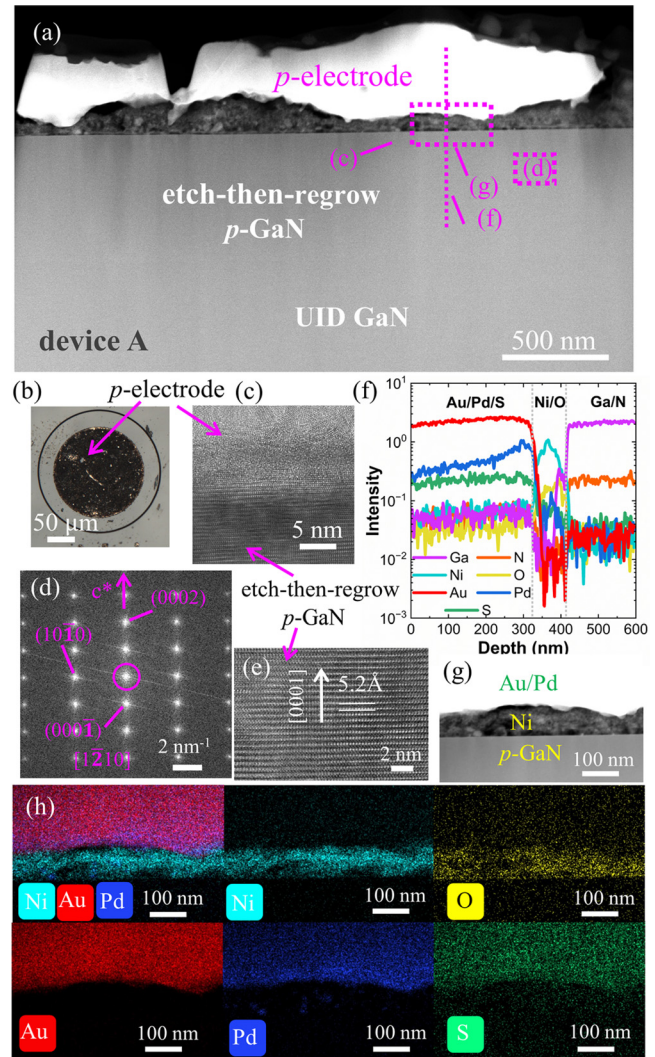


FIG. 3. Microscopy investigation of device A after the Venus test. (a) FIB cross section image of the device. (b) Optical image of p -electrode. (c) Zoom-in view of p -electrode contacts with regrown p -GaN. (d) Crystallinity (reciprocal lattice, FFT of TEM) of etch-then-regrown p -GaN. (e) HRTEM image of etch-then-regrown p -GaN. (f) EDX spectra along the pink dash line in (a). (g) HAADF-STEM of p -electrode contacts with p -GaN. (h) Compositional EDX elemental mapping of Au, Ni, Pd, Ga, N, S, and O (FIB: focused ion beam; FFT: fast Fourier transform; HRTEM: high resolution TEM; HAADF-STEM: high-angle annular dark-field scanning TEM; EDX: energy-dispersive x-ray spectroscopy).

Venus test is mainly due to *p*-electrode's degradation, which further supports the Schottky/*p-n* diode model proposed in this work.

Despite the existence of the Schottky contact after the Venus test, both devices maintain rectification behavior up to 500 °C. Specifically, a current density of ~12.5 A/cm² and a rectification factor of ~10⁶ at 6 V are achieved [Fig. 4(a)]. Meanwhile, the reverse leakage current is larger in device A than that in device B. *C-V* measurements at various frequencies after the Venus test provide a possible explanation for this phenomenon. The capacitance decreases with increasing frequency [Figs. 4(b) and 4(c)], which has been reported in similar GaN *p-n* diodes.²³ The frequency dispersion of the capacitance is an indicator of defects or interfaces distributed in the devices. Defects or interfaces' effects on capacitance are negligibly small at high frequency since most of them cannot follow the *ac* signal.

For reverse bias, a larger frequency dispersion is observed in device A than device B, indicating much higher defect density in the etch-then-regrow device [Fig. 4(c)]. The *C-V* trends are different at negative bias between device A and device B, and the capacitance of device A is larger. The authors have reported that the etch-then-regrow interface could have a high positive charge concentration on the order

of 10¹⁷–10²⁰ cm⁻³.²³ Such high charge concentration contributes to the large reverse leakage currents, which could explain a larger reverse leakage current in device A under high temperature [Fig. 4(a)].

Using the parallel-plate capacitor model, the relationship between capacitance and depletion width is $C_d = \frac{\epsilon_0 \epsilon_{\text{GaN}}}{W_d}$, where C_d is the capacitance per unit area, ϵ_0 is the vacuum dielectric constant, ϵ_{GaN} is the relative dielectric constant of GaN and is assumed to be 8.9 in this work, and W_d is the depletion width. For device A, since its etched surface is heavily doped, the depletion width is shorter than that of device B under the same bias [Fig. 4(d)]. Consequently, the capacitance of device A is larger under the same bias. The decreased capacitance at forward bias occurs in both devices, which could be attributed to *p*-electrode/*p*-GaN Schottky junction capacitance [Fig. 4(d)]. This further supports the Schottky/*p-n* diode model proposed in this work. Using a one-side abrupt junction model for device B, the relationship between capacitance and doping concentration is expressed as $\frac{d(1/C_d^2)}{dV} = \frac{-2}{q\epsilon_0\epsilon_{\text{GaN}}(N_D^+ - N_A^+ + N_t)}$, where N_D^+ is the ionized donor concentration, N_A^+ is the ionized acceptor concentration, and N_t is the equivalent charge concentration of traps.³⁸ According to the above-mentioned equation, the charge concentration of UID GaN is on the order of 10¹⁵ cm⁻³ in device B, which proves that the one-side abrupt junction model is reasonable for device B [Fig. 4(f)]. This charge concentration is of the same order as mentioned in our previous report without exposure to extreme environments.²³ For device A, the depletion width is approximately 1.1 μm at 10 kHz and negative bias [Fig. 4(e)]. The space charge region is mainly located at the *p*-GaN layer and the etch-then-regrow interface. Since the etch-then-regrow interface is equivalent to n⁺ doping, the length of the space charge region increases slowly at reverse bias [Fig. 4(e)].

This work investigates the robustness of the vertical GaN devices at a highest temperature of 500 °C.^{39–43} Specifically, this work reports the 500 °C properties of vertical GaN *p-n* diodes with regrown *p*-GaN after extreme environment exposure. Sulfurization of the *p*-electrode, which leads to a Schottky/*p*-GaN interface, has been identified as the main degradation mechanism after exposure to extreme environments. In the broader context, this result has significant implications for GaN devices for operation in extreme environments. Suitable passivation, such as SiO₂ and multilayer dielectrics (Al₂O₃/SiO₂/SiON), for the metallization regions could be introduced.^{31,44} These improvements would allow for further study of the thermal robustness of the intrinsic *p-n* diodes. Furthermore, for vertical GaN *p-n* diodes, an improved etch-then-regrow processes (e.g., reducing etching rate^{13,14}) would further improve the performance of these devices and their reliability in harsh environments.

In summary, this work investigates the high-temperature performances of the vertical GaN *p-n* diodes with regrown *p*-GaN after exposure to the simulated Venus environment. Comprehensive electrical characterization and microscopy investigation revealed that *p*-electrode degradation is the main degradation of the device performance after extreme environment exposure. These results are an important reference for GaN vertical power devices' operation in extreme environments.

This work was supported in part by NASA HOTTech Program under Award No. 80NSSC17K0768, in part by ULTRA, an Energy Frontier Research Center funded by the U.S. Department of Energy

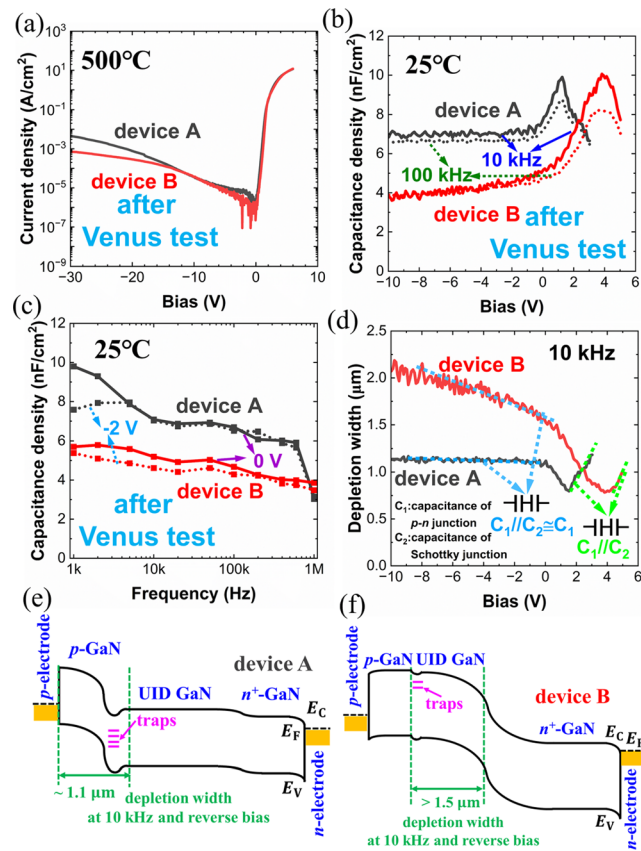


FIG. 4. (a) *J-V* characteristic of device A at 500 °C after the Venus test. (a) *C-V* curves at 10 and 100 kHz for device A and B after the Venus test. (b) *C-f* curves at -2 and 0 V for device A and B after the Venus test. (c) Depletion width with bias at 10 kHz for device A and B after the Venus test. (d) Doping profile extracted from the *C-V* curve at 10 kHz for device B. Schematic of energy band structure and depletion region at 10 kHz and negative bias for (e) device A and (f) device B.

(DOE), Office of Science, Basic Energy Sciences (BES), under Award No. DE-SC0021230, in part by CHIMES, one of the seven centers in JUMP 2.0, a Semiconductor Research Corporation (SRC) program sponsored by DARPA, in part by the NanoFab through NSF under Award No. ECCS-1542160, in part by the National Science Foundation (NSF) under Award No. 2302696, in part by the National Science Foundation (NSF) under Award No. DMR-2005096, in part by OPEN 2021 ARPA-E program under Award No. DE-AR0001591, and in part by AFOSR under Award No. FA9550-22-1-0367. The authors would like to acknowledge the use of facilities within the Eyring Materials Center at Arizona State University, the use of GEER at NASA, and the use of Electron Microscopy Center, Shared Equipment Authority at Rice University. The device fabrication was performed at the Center for Solid Electronics Research at Arizona State University.

AUTHOR DECLARATIONS

Conflict of Interest

The authors have no conflicts to disclose.

Author Contributions

Shisong Luo: Conceptualization (equal); Data curation (lead); Formal analysis (lead); Investigation (lead); Methodology (lead); Validation (equal); Visualization (equal); Writing – original draft (equal); Writing – review & editing (equal). **Zhaobo Mei:** Conceptualization (equal); Formal analysis (equal); Investigation (equal); Methodology (equal); Visualization (equal); Writing – review & editing (equal). **Mingfei Xu:** Conceptualization (equal); Investigation (equal); Methodology (equal); Writing – review & editing (equal). **Jingan Zhou:** Conceptualization (equal); Investigation (equal); Methodology (equal); Writing – review & editing (equal). **Ziyi He:** Conceptualization (equal); Investigation (equal); Methodology (equal); Writing – review & editing (equal). **Cheng Chang:** Conceptualization (supporting); Investigation (supporting); Methodology (supporting); Writing – review & editing (supporting). **Hanyu Zhu:** Conceptualization (equal); Investigation (equal); Methodology (equal); Resources (supporting); Writing – review & editing (equal). **Tomás Palacios:** Conceptualization (equal); Formal analysis (equal); Funding acquisition (equal); Investigation (equal); Methodology (equal); Supervision (equal); Writing – original draft (equal); Writing – review & editing (equal). **Yuji Zhao:** Conceptualization (equal); Data curation (equal); Formal analysis (equal); Funding acquisition (lead); Investigation (equal); Methodology (equal); Project administration (lead); Resources (equal); Software (equal); Supervision (lead); Validation (equal); Visualization (equal); Writing – original draft (equal); Writing – review & editing (equal). **Qingyun Xie:** Conceptualization (equal); Formal analysis (equal); Investigation (equal); Methodology (equal); Writing – review & editing (equal). **Mengyang Yuan:** Conceptualization (equal); Investigation (equal); Methodology (equal); Writing – review & editing (equal). **Guanhui Gao:** Conceptualization (equal); Formal analysis (equal); Investigation (equal); Methodology (equal); Validation (equal); Visualization

(equal); Writing – review & editing (equal). **Hua Guo:** Conceptualization (equal); Investigation (equal); Methodology (equal); Visualization (equal); Writing – review & editing (equal). **Rui Xu:** Conceptualization (equal); Investigation (equal); Methodology (equal); Resources (supporting); Writing – review & editing (equal). **Noah Giles:** Conceptualization (equal); Investigation (equal); Methodology (equal); Writing – review & editing (equal). **Tao Li:** Conceptualization (equal); Investigation (equal); Methodology (equal); Visualization (supporting); Writing – review & editing (equal).

DATA AVAILABILITY

The data that support the findings of this study are available from the corresponding author upon reasonable request.

REFERENCES

- P. G. Neudeck, R. S. Okojie, and L. Y. Chen, *Proc. IEEE* **90**(6), 1065 (2002).
- S. Jones-Jackson, R. Rodriguez, and A. Emadi, *IEEE Trans. Power Electron.* **36**(9), 10420 (2021).
- L. Dorn-Gomba, J. Ramoul, J. Reimers, and A. Emadi, *IEEE Trans. Transp. Electrification* **6**(4), 1648 (2020).
- A. Hassan, Y. Savaria, and M. Sawan, *IEEE Trans. Very Large Scale Integr. (VLSI) Syst.* **26**(10), 2085 (2018).
- Q. Xie, M. Yuan, J. Niroula, B. Sikder, S. Luo, K. Fu, N. S. Rajput, A. B. Pranta, P. Yadav, Y. Zhao, N. Chowdhury, and T. Palacios, in *Symposium on VLSI Technology and Circuits* (IEEE, 2023), p. 1–2.
- M. Sadek, S. Han, J. Song, J. C. Gallagher, T. J. Anderson, and R. Chu, *IEEE Trans. Electron Devices* **69**(4), 1912 (2022).
- D. Khachariya, S. Stein, W. Mecouch, M. H. Breckenridge, S. Rathkantiwar, S. Mita, B. Moody, P. Reddy, J. Tweedie, R. Kirste, K. Sierakowski, G. Kamler, M. Bockowski, E. Kohn, S. Pavlidis, R. Collazo, and Z. Sitar, *Appl. Phys. Express* **15**(10), 101004 (2022).
- R. Zhang, Y. Liu, Q. Li, S. Pidaparathi, A. Edwards, C. Drowley, and Y. Zhang, *IEEE Electron Device Lett.* **43**(3), 366 (2022).
- K. Fu, Z. He, C. Yang, J. Zhou, H. Fu, and Y. Zhao, *Appl. Phys. Lett.* **121**, 092103 (2022).
- H. Fu, K. Fu, S. Chowdhury, T. Palacios, and Y. Zhao, *IEEE Trans. Electron Devices* **68**(7), 3200 (2021).
- H. Fu, K. Fu, S. Chowdhury, T. Palacios, and Y. Zhao, *IEEE Trans. Electron Devices* **68**(7), 3212 (2021).
- R. Hoo Teo, Y. Zhang, N. Chowdhury, S. Rakheja, R. Ma, Q. Xie, E. Yagyu, K. Yamanaka, K. Li, and T. Palacios, *J. Appl. Phys.* **130**(16), 160902 (2021).
- H. Fu, K. Fu, C. Yang, H. Liu, K. A. Hatch, P. Peri, D. H. Mudiyansele, B. Li, T. Kim, S. R. Alugubelli, P. Su, D. C. Messina, X. Deng, C. Cheng, R. V. Meidanshahi, X. Huang, H. Chen, T. Yang, J. Zhou, A. M. Armstrong, A. A. Allerman, E. T. Yu, J. Han, S. M. Goodnick, D. J. Smith, R. J. Nemanich, F. A. Ponce, and Y. Zhao, *Mater. Today* **49**, 296 (2021).
- K. Fu, H. Fu, X. Huang, H. Chen, T. Yang, J. Montes, C. Yang, J. Zhou, and Y. Zhao, *IEEE Electron Device Lett.* **40**(11), 1728 (2019).
- C. Yang, H. Fu, V. N. Kumar, K. Fu, H. Liu, X. Huang, T. Yang, H. Chen, J. Zhou, X. Deng, J. Montes, F. A. Ponce, D. Vasileksa, and Y. Zhao, *IEEE Trans. Electron Devices* **67**(10), 3972 (2020).
- H. Liu, H. Fu, K. Fu, S. R. Alugubelli, P. Su, Y. Zhao, and F. A. Ponce, *Appl. Phys. Lett.* **114**, 082102 (2019).
- P. Su, H. Liu, C. Yang, K. Fu, H. Fu, Y. Zhao, and F. A. Ponce, *Appl. Phys. Lett.* **117**, 102110 (2020).
- A. S. Chang, B. Li, S. Wang, M. Nami, P. J. M. Smeets, J. Han, and L. J. Lauhon, *ACS Appl. Electron. Mater.* **3**(2), 704 (2021).
- B. Li, S. Wang, M. Nami, A. M. Armstrong, and J. Han, *ACS Appl. Mater. Interfaces* **13**(44), 53220 (2021).
- A. S. Chang, B. Li, S. Wang, S. Frisone, R. S. Goldman, J. Han, and L. J. Lauhon, *Nano Energy* **102**, 107689 (2022).
- R. A. Ferreyra, B. Li, S. Wang, and J. Han, *J. Phys. D* **56**, 373001 (2023).

- ²²H. Fu, K. Fu, H. Liu, S. R. Alugubelli, X. Huang, H. Chen, J. Montes, T. Yang, C. Yang, J. Zhou, F. A. Ponce, and Y. Zhao, *Appl. Phys. Express* **12**, 051015 (2019).
- ²³K. Fu, H. Fu, H. Liu, S. R. Alugubelli, T. Yang, X. Huang, H. Chen, I. Baranowski, J. Montes, F. A. Ponce, and Y. Zhao, *Appl. Phys. Lett.* **113**, 233502 (2018).
- ²⁴K. Fu, X. Qi, H. Fu, P. Su, H. Liu, T. Yang, C. Yang, J. Montes, J. Zhou, F. A. Ponce, and Y. Zhao, *Semicond. Sci. Technol.* **36**, 014005 (2020).
- ²⁵P. Peri, K. Fu, H. Fu, Y. Zhao, and D. J. Smith, *J. Electron. Mater.* **50**(5), 2637 (2021).
- ²⁶K. Fu, H. Fu, X. Deng, P. Su, H. Liu, K. Hatch, C. Cheng, D. Messina, R. V. Meidanshahi, P. Peri, C. Yang, T. Yang, J. Montes, J. Zhou, X. Qi, S. M. Goodnick, F. A. Ponce, D. J. Smith, R. Nemanich, and Y. Zhao, *Appl. Phys. Lett.* **118**, 222104 (2021).
- ²⁷T. Kim, K. Fu, C. Yang, Y. Zhao, and E. T. Yu, *J. Appl. Phys.* **131**, 015704 (2022).
- ²⁸A. M. Fischer, S. Wang, F. A. Ponce, B. P. Gunning, C. A. M. Fabien, and W. A. Doolittle, *Phys. Status Solidi B* **254**(8), 1600668 (2017).
- ²⁹M. H. Breckenridge, J. Tweedie, P. Reddy, Y. Guan, P. Bagheri, D. Szymanski, S. Mita, K. Sierakowski, M. Boćkowski, R. Collazo, and Z. Sitar, *Appl. Phys. Lett.* **118**(2), 022101 (2021).
- ³⁰T. Kremic, D. Vento, N. Lalli, and T. Palinski, in *2014 IEEE Aerospace Conference* (IEEE, 2014), p. 1–9.
- ³¹M. Yuan, J. Niroula, Q. Xie, N. S. Rajput, K. Fu, S. Luo, S. K. Das, A. J. B. Iqbal, B. Sikder, M. F. Isamotu, M. Oh, S. R. Eisner, D. G. Senesky, G. W. Hunter, N. Chowdhury, Y. Zhao, and T. Palacios, *IEEE Electron Device Lett.* **44**(7), 1068 (2023).
- ³²E. H. Rhoderick and R. H. Williams, *Metal Semiconductor Contacts*, 2nd ed. (Oxford University Press, Oxford, 1988).
- ³³J. M. Shah, Y. L. Li, T. Gessmann, and E. F. Schubert, *J. Appl. Phys.* **94**(4), 2627 (2003).
- ³⁴E. F. Chor, D. Zhang, H. Gong, G. L. Chen, and T. Y. F. Liew, *J. Appl. Phys.* **90**(3), 1242 (2001).
- ³⁵I. Levchenko, S. Kryvyi, E. Kamińska, S. Grzanka, E. Grzanka, Ł. Marona, and P. Perlin, *Materials* **16**(19), 6568 (2023).
- ³⁶D. Lukco, D. J. Spry, R. P. Harvey, G. C. C. Costa, R. S. Okojie, A. Avishai, L. M. Nakley, P. G. Neudeck, and G. W. Hunter, *Earth Space Sci.* **5**(7), 270 (2018).
- ³⁷P. G. Neudeck, L. Chen, R. D. Meredith, D. Lukco, D. J. Spry, L. M. Nakley, and G. W. Hunter, *IEEE J. Electron Devices Soc.* **7**, 100 (2019).
- ³⁸S. M. Sze and K. K. Ng, *Physics of Semiconductor Devices*, 3rd ed. (John Wiley & Sons, Inc., 2007).
- ³⁹X. Zou, X. Zhang, X. Lu, C. W. Tang, and K. M. Lau, *IEEE Electron Device Lett.* **37**(9), 1158 (2016).
- ⁴⁰J. Liu, R. Zhang, M. Xiao, S. Pidaparathi, H. Cui, A. Edwards, L. Baubutr, C. Drowley, and Y. Zhang, *IEEE Trans. Power Electron.* **36**(10), 10959 (2021).
- ⁴¹B. Shankar, K. Zeng, B. Gunning, R. P. Martinez, C. Meng, J. Flicker, A. Binder, J. R. Dickerson, R. Kaplar, and S. Chowdhury, in *2022 Device Research Conference (DRC)* (IEEE, 2022), Vol. 69, p. 1–2.
- ⁴²J. Liu, M. Xiao, R. Zhang, S. Pidaparathi, H. Cui, A. Edwards, M. Craven, L. Baubutr, C. Drowley, and Y. Zhang, *IEEE Trans. Electron Devices* **68**(4), 2025 (2021).
- ⁴³K. Fu, S. Luo, H. Fu, K. Hatch, S. R. Alugubelli, H. Liu, T. Li, M. Xu, Z. Mei, Z. He, J. Zhou, C. Chang, F. A. Ponce, R. Nemanich, and Y. Zhao, *IEEE Trans. Electron Devices* **1**, 1–5 (2023).
- ⁴⁴H. Lee, H. Ryu, and W. Zhu, *Appl. Phys. Lett.* **122**, 112103 (2023).